COMMUNICATION www.rsc.org/chemcomm | ChemComm

A green process for coupling manganese oxides with titanium(IV) dioxide†

Nanae Nishimura,[a] Jyunya Tanikawa,[a] Masashi Fujii,[a] Tetsuro Kawahara,*[b] Juichi Ino,*[b] Tomoki Akita,[c] Takayoshi Fujino[a] and Hiroaki Tada*[a]

Received (in Cambridge, UK) 7th March 2008, Accepted 2nd May 2008
First published as an Advance Article on the web 9th June 2008
DOI: 10.1039/b803989e

MnO_2 nanoparticle-loaded TiO_2 prepared by a green process capable of removing harmful MnO_4^- ions from water exhibits catalytic activity for a test reaction, H_2O_2 decomposition, in the dark with its activity enhanced by UV light irradiation.

Increasing air and water pollution demands us to develop environmental purification catalysts, among which is metal-oxide semiconductor photocatalysts represented by TiO_2 having a photoinduced oxidation power strong enough to completely mineralize organic pollutants.[1,2] A major problem of semiconductor photocatalysis is the low reaction efficiency due to the fast recombination of photogenerated charge carriers. The coupling of semiconductor photocatalysts with metal nanoparticles,[3,4] different semiconductors,[5–9] and the both[10] is a promising approach to improve the charge separation efficiency through interfacial electron transfer. Another serious problem from a practical viewpoint is that photocatalysts are entirely inactive in the dark, which severely restricts their use. On the other hand, MnO_2 is known to exhibit thermally activated catalytic activity for the oxidation of organic pollutants,[11] although it falls short of the photocatalytic activity of TiO_2. Thus, if MnO_2 can be appropriately coupled with TiO_2, this heterostructured system would act as a powerful environmental catalyst working with and without light. In this case, the synthetic route should also be environmentally benign. $KMnO_4$ contained in waste water from nonferrous metal manufactures causes water pollution because of its strong toxicity for aquatic life.[12]

Here we report a green process for preparing MnO_2 nanoparticle (NP)-loaded TiO_2 particles (MnO_2/TiO_2), further showing the complementary effects of MnO_2/TiO_2 on the (photo)catalytic activities for the decomposition of H_2O_2 employed as a model pollutant. Manganese oxide was loaded on anatase TiO_2 particles by a novel photodeposition method.‡ Fig. 1 shows the electronic absorption spectral change of deaerated aqueous $KMnO_4$ solutions with irradiation ($\lambda_{ex} > 300$ nm) in the absence (A) and presence (B) of TiO_2: initial $KMnO_4$ concentration ($[KMnO_4]_0$) = 1 mmol dm^{-3}, and the initial pH (pH_0) 7. The aqueous solution of $KMnO_4$ has two broad absorptions centred at 300 (B_1) and 550 nm (B_2). These two absorption bands are characterized by quantum chemical calculations as the excitations from the nonbonding orbitals of oxygen to the antibonding orbitals between metal and oxygens.[13] When the $KMnO_4$ solution was irradiated without TiO_2 (Fig. 1(A)), the absorption intensity below 500 nm increases, whereas that of B_2 is almost invariant. No precipitates were observed even after 3 h irradiation. Partial photodecomposition of MnO_4^- ions to MnO_4^{2-} ions and O_2[14] seems to be responsible for the spectral change. On the other hand, with TiO_2 (Fig. 1(B)), both the absorption intensities of B_1 and B_2 rapidly decrease. This drastic difference in the spectral change between (A) and (B) suggests that a distinct reaction takes place in the presence of TiO_2, and the self-photoreduction of MnO_4^- ions is negligible under the conditions.

After 2 h irradiation to a 1.74 mmol dm^{-3} $KMnO_4$ solution containing TiO_2 particles (3.0 g), they were recovered by centrifugation, and the same procedures were repeated n times. Transmission electron microscopic (TEM) observation and

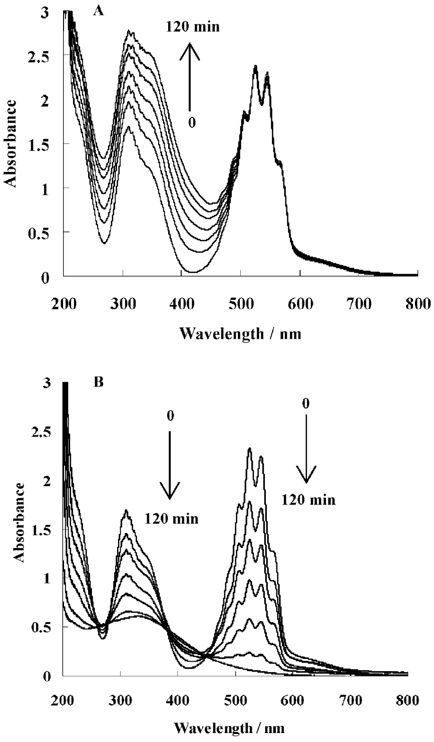

Fig. 1 Electronic absorption spectral change of an aqueous solution of $KMnO_4$ with irradiation ($\lambda_{ex} > 300$ nm) without (A) and with TiO_2 (B): $[KMnO_4]_0$ = 1 mmol dm^{-3}; pH_0 7.

---

[a] *Department of Applied Chemistry, Faculty of Science and Engineering, Kinki University, 3-4-1 Kowakae, Higashi-Osaka, Osaka, 577-8502, Japan. E-mail: h-tada@apch.kindai.ac.jp; Fax: +81-6-6727-4301; Tel: +81-6-6721-2332*
[b] *Nippon Sheet Glass Co. Ltd., 2-13-12, Konoike, Itami, Hyogo, 664-8520, Japan. E-mail: TetsuroKawahra@mail.nsg.co.jp;JuichiIno@mail.nsg.co.jp; Fax: +81-72-779-6906; Tel: +81-72-781-0081*
[c] *National Institute of Advanced Industrial Science and Technology, Midorigaoka 1-8-31, Ikeda, Osaka, 563-8577, Japan*

† Electronic supplementary information (ESI) available: Fig. S1: Electronic absorption spectra of β-$MnO_2(n)/TiO_2$ (n = 0, 1, 2, 3, 5). Fig. S2: Time courses for CH_3CHO decomposition in the dark and under irradiation for TiO_2 and for β-$MnO_2(5)/TiO_2$. Table S1: XPS binding energies for as-deposited and heated samples of β-$MnO_2(5)/TiO_2$. See DOI: 10.1039/b803989e

electron energy loss spectroscopic (EELS) measurements were carried out for a sample ($n = 5$). Fig. 2(A) and (B) show TEM images for as-deposited and heated samples, respectively: heating conditions, 873 K for 2 h. The shape of nanometer-sized particles (NPs) deposited on the TiO_2 surface changes from stick-like to cubic as a result of the heat treatment. Fig. 2(C) compares O K-edge structures of EELS obtained for as-deposited and heated samples by an irradiating electron beam focused on locations (a) and (b) in Fig. 2(A) and (B), respectively.[15] The profiles of the spectra are quite different, and spectra (a) and (b) resemble those of Mn_3O_4 and MnO_2, respectively. Also, a high-resolution (HR)-TEM image (Fig. 2(D)) shows clear crystal-lattice fringes, for which distances are in agreement with those of the (101) and (110) planes of β-MnO_2 (ICDD No. 24-0735).

X-Ray photoelectron spectroscopic (XPS) measurements for the heated sample provided a Mn $2p_{3/2}$ binding energy of 642.5 eV, which is close to the value reported for β-MnO_2 (642.6 eV) (Table S1, ESI†).[16] On the other hand, the fact that the Mn $2p_{3/2}$ binding energy for the as-deposited sample is lower (642.3 eV) is consistent with the conclusion that the deposits are Mn_3O_4. Also, the surface atom% ratio of Mn/Ti decreased from 0.29 to 0.15 with the heat treatment. This indicates the increase in the degree of the surface exposure of TiO_2, reflecting the change in the number density and morphology of the deposits with heating. As a result of β-MnO_2 loading, broad absorption due to d–d transition appears in the visible region[17] with its intensity increased with increasing n, whereas TiO_2 has only absorption below 385 nm (Fig. S1 in ESI†). Evidently, UV-light irradiation to aqueous $KMnO_4$ solutions in the presence of TiO_2 particles leads to the deposition of stick-shaped Mn_3O_4 NPs, which are changed to cubic β-MnO_2 by heating at 873 K for 2 h.

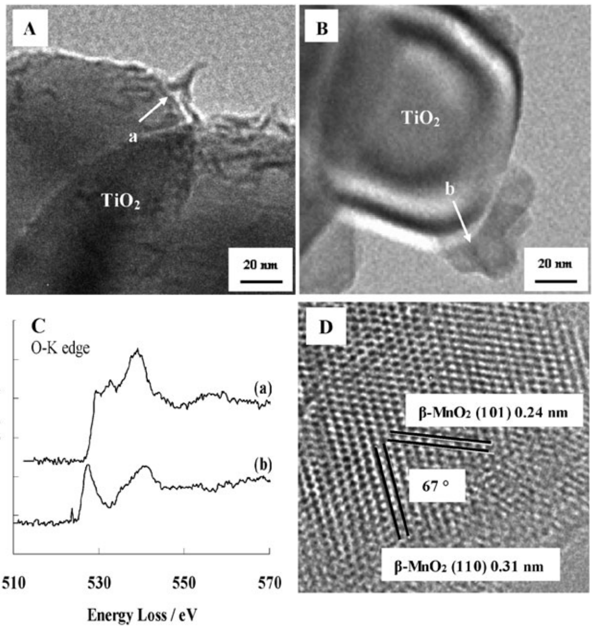

Fig. 2 TEM images for as-deposited (A) and heated samples (B). (C) EELS for as-deposited (a) and heated samples (b). D, HRTEM image of the heated sample.

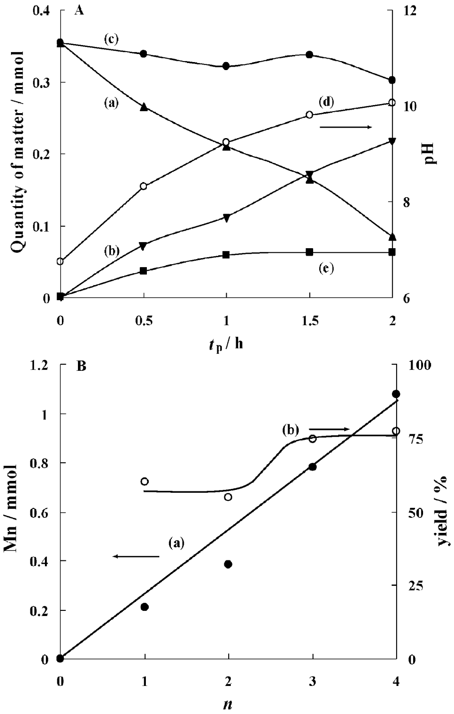

Fig. 3 (A) The material balance of the reaction: (a) Mn remaining in the solution; (b) Mn deposited on TiO_2; (c) total Mn amount; (d) pH; (e) O_2. (B) Plots of the amount of Mn deposited and the yield *vs.* n.

The material balance of the reaction was checked. Fig. 3(A) shows the amounts of reactant and products, and pH as a function of t_p. The sum of the amount of Mn remaining in the solution (a) and that deposited on TiO_2 (b) is almost equal to the total amount (c) irrespective of t_p, which indicates that MnO_4^- is quantitatively removed from the solution. Upon irradiation, the pH (d) of the solution increases concurrently with the generation of O_2 (e). The ratio of the amount of MnO_4^- decreased (0.27 mmol) to that of O_2 generated (0.081 mmol) is *ca.* 3 at $t_p = 2$ h. Thus, the overall photodeposition of Mn_3O_4 can be written by eqn (1).

$$3\mathrm{MnO_4^-} + 12\mathrm{H^+} \xrightarrow{\mathrm{TiO_2},h\nu} \mathrm{Mn_3O_4} + 6\mathrm{H_2O} + \mathrm{O_2} \qquad (1)$$

On the basis of these results, the essential mechanism on this reaction is summarized as follows. UV light irradiation to TiO_2 gives rise to excitation of electrons in the valence band (vb) to the conduction band (cb). In the cathodic process, MnO_4^- ions having strong oxidation power effectively accept the excited electrons from TiO_2 to be deposited as Mn_3O_4 NPs on the surface (Mn_3O_4/TiO_2). In the anodic process, the holes left in the vb oxidize adsorbed H_2O to produce H^+ and O_2. Further, Mn_3O_4 NPs are changed to β-MnO_2 NPs by heating at 873 K. Photodeposition of various metal particles[3,4] and chalcogenides[6] on semiconductors *via* the photocatalytic reduction process is well known; however, metal oxide photodeposition is limited to those of Cu_2O on TiO_2 from Cu^{2+} ions[18] and $Cr(OH)_3$ from Cr^{6+} ions on TiO_2,[19] and Co_3O_4 from Co^{2+} ions on ZnO.[20] Fig. 3(B) shows the amount of Mn deposited from the aqueous solution (a) and the yield (b) as a function of n. The amount of Mn deposited increases in proportion to n, and each yield after 2 h irradiation ranges between 60 and 75%. Further, it was confirmed by inductively coupled plasma spectroscopy that the MnO_4^- ions in the solution is almost completely removed at $t_p \geq 2.5$ h. Thus, this method is useful for the removal of MnO_4^- ions from water as well as a technique of MnO_2–TiO_2 coupling.

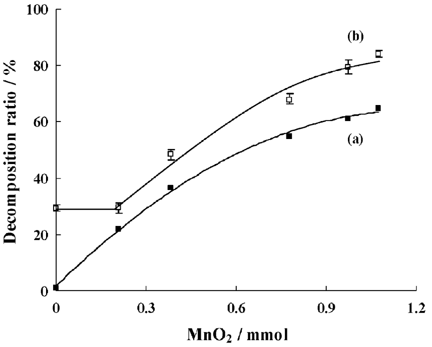

Fig. 4 (Photo)catalytic activities of β-MnO_2/TiO_2 for H_2O_2 decomposition in the dark (a) and under irradiation (b).

The decomposition of H_2O_2, widely used as a test catalytic reaction,[21] is also of importance for waste water treatment in semiconductor industries.[22] Fig. 4 shows the decomposition ratio of H_2O_2 (reaction time = 1 h) in the presence of β-MnO_2/TiO_2 in the dark and under UV light irradiation ($\lambda_{ex} > 300$ nm). In the dark, β-MnO_2/TiO_2 exhibits catalytic activity for the H_2O_2 decomposition of which the rate increases with an increase in the loading amount of β-MnO_2, whereas TiO_2 is inactive by itself. The generation of O_2 during this reaction was confirmed using an O_2 meter. Interestingly, irradiation accelerates the decomposition in every case, and more than 80% of H_2O_2 is decomposed with β-MnO_2(1.1 mass%)/TiO_2 after only 1 h irradiation. H_2O_2 can be decomposed by both cb-electrons and vb-holes in TiO_2.[23] In the former, H_2O_2 are reduced to OH^- and $^\bullet OH$, while in the latter, H_2O_2 are oxidized to produce O_2^-. This finding demonstrates the complementary effect of thermally activated active MnO_2 and TiO_2 photocatalyst for the decomposition of H_2O_2. The (photo)catalytic activities of β-MnO_2/TiO_2 for the decomposition of CH_3CHO, a common indoor air pollutant, were examined as an additional test reaction (Fig. S2, ESI†). From the experiments at room temperature in the dark, the decreases in the CH_3CHO concentration due to adsorption for 1 h in the TiO_2 and β-MnO_2/TiO_2 systems were found to be below 30 ppm. Even in the dark at 423 K, TiO_2 showed a catalytic activity, which slightly increased with irradiation. Interestingly, the catalytic activities in the dark and under irradiation significantly increased with loading 2.47 mass% of β-MnO_2. These findings also indicate the synergy effect of β-MnO_2 and TiO_2. The optimization of the size and distribution of β-MnO_2 NPs could increase the catalytic activity.[11]

In summary, manganese oxide-coupled TiO_2 was prepared by a green process capable of removing harmful MnO_4^- ions from water. β-MnO_2/TiO_2 prepared by post-heating exhibited catalytic activity for the H_2O_2 decomposition in the dark, which was enhanced with UV light irradiation. This coupled system can be expected to apply to not only water purification but air purification.

Notes and references

‡ Anatase TiO_2 particles having a specific surface are of 8.1 $m^2 g^{-1}$ (3 g, A-100, Ishihara Techno Co.) were suspended in a $KMnO_4$ aqueous solution set to pH 7 with NaOH aq. The initial concentration of $KMnO_4$ was 1.74 mmol dm^{-3} unless otherwise noted in the text. After the suspension in a double-jacket type reaction cell had been purged with Ar for 0.5 h, UV light irradiation ($\lambda_{ex} > 300$ nm, $I_{310-400}$ nm = 8.5 mW cm^{-2}) was started using a 400 W high-pressure mercury arc (H-400P, Toshiba) with Ar-bubbing and stirring continued throughout the irradiation. The reaction temperature was kept at 298 K by circulating thermostated water through the outer jacket around the cell. After irradiation, the particles were recovered by centrifugation, and these procedures were repeated *n* times. The resulting particles were washed with distilled water, dried under vacuum, and then heated at 873 K in air for 2 h. The manganese oxides deposited TiO_2 particles were completely dissolved by treating the particles (0.1 g) with 10 mL aqua regia. After the solution had been diluted to 50 mL with water, the amount of Mn was determined by inductively coupled plasma spectroscopy (ICPS-7500, Shimadzu). The electronic absorption spectra of the $KMnO_4$ solutions and the particles were measured by UV/Vis spectroscopy (U-4000, Hitachi). HRTEM observation and EELS measurements were performed using a JEOL JEM-3000F and Gatan Imaging Filter at an applied voltage of 300 or 297 kV at an applied voltage of 300 kV. Catalytic activities of β-MnO_2/TiO_2 for the decomposition of H_2O_2 were examined in the dark and under irradiation ($\lambda_{ex} > 300$ nm, $I_{310-400}$ nm = 4.0 mW cm^{-2}) using the same experimental set up in the photodeposition of manganese oxides. β-MnO_2/TiO_2 particles (50 mg) were dispersed in a 4 mmol dm^{-3} H_2O_2 aqueous solution. UV light was irradiated to the suspension in a double-jacket type reaction cell with stirring. In both the dark and photocatalytic reactions, the cell temperature was kept at 298 K by circulating thermostated water through the outer jacket around the cell. After 1 h, the suspension was filtered and conc. H_2SO_4 (1.25 mL) was added to the filtrate (5 mL), and the concentration of H_2O_2 in the solution was determined by $KMnO_4$ titration. Also, the change in the O_2 concentration in the solution was traced using an O_2 meter (DO-11P, Toadenpa Kogyo Co.). The (photo)catalytic activities were evaluated also for gas-phase oxidation of CH_3CHO. The sample (50 mg) was spread in a stainless holder (30 mm ϕ) and placed in a vacuum chamber. A 500 ppm standard CH_3CHO gas (balance: N_2) was introduced into it and diluted with air such that its initial concentration was kept *ca.* 320 ppm. The reaction was run at 423 K in the dark and under irradiation ($\lambda > 300$ nm, $I_{320-400}$ = 3.0 mW cm^{-2}) using a 300-W xenon lamp (Wacom, HX-500). The concentration of CH_3CHO was determined by gas chromatography (Shimadzu, GC-2014) with an f.i.d. column SHINCARBON A (3 mmϕ × 3 m).

1. K. Hashimoto, H. Irie and A. Fujishima, *Jpn. J. Appl. Phys.*, 2005, **44**, 8269.
2. C. G. Granqvist, A. Azens, P. Heszler, L. B. Kish and L. Osterlund, *Sol. Energy Mater. Sol. Cells*, 2007, **91**, 355.
3. P. D. Cozzoli, E. Fanizza, R. Comparelli, M. Curri, A. Lucia, A. Agostiano and D. Laub, *J. Phys. Chem. B*, 2004, **108**, 9623.
4. V. Subramanian, E. E. Wolf and P. V. Kamat, *J. Am. Chem. Soc.*, 2004, **126**, 4943.
5. K. Rajeshwar, N. R. De Tacconi and C. R. Chenthamarakshan, *Chem. Mater.*, 2001, **13**, 2765.
6. V. N. H. Nguyen, R. Amal and D. Beydoun, *J. Photochem. Photobiol. A: Chem.*, 2006, **179**, 57–65.
7. H. Tada, A. Hattori, Y. Tokihisa, K. Imai, N. Tohge and S. Ito, *J. Phys. Chem. B*, 2000, **104**, 4585.
8. S. Daxin, F. Yaqing and Z. Shunhe, *Catal. Today*, 2004, **98**, 505.
9. M. Long, W. Cai and H. Kisch, *J. Phys. Chem. C*, 2008, **112**, 548.
10. H. Tada, T. Mitsui, T. Kiyonaga, T. Akita and K. Tanaka, *Nat. Mater.*, 2006, **5**, 702.
11. A. K. Sinha, K. Suzuki, M. Takahara, H. Azuma, T. Nonaka and K. Fukumoto, *Angew. Chem., Int. Ed.*, 2007, **46**, 2891.
12. *Commission of European Communities*, Luxumbourg, 1993, p. 125.
13. H. Nakai, Y. Ohmori and H. Nakatsuji, *J. Chem. Phys.*, 1991, **95**, 8287.
14. D. G. Lee, C. R. Moylan, T. Hayashi and J. I. Brauman, *J. Am. Chem. Soc.*, 1987, **109**, 3003.
15. H. Kurata and C. Colliex, *Phys. Rev. B.*, 1993, **48**, 2102.
16. C. Poisignon, G. Berthome, B. Prelot, F. Thomas and F. Villieras, *J. Electrochem. Soc.*, 2004, **151**, A1611.
17. N. Sakai, Y. Ebina, K. Takada and T. Sasaki, *J. Phys. Chem. B*, 2005, **109**, 9651.
18. J. W. M. Jacobs, F. W. H. Kampers, J. M. G. Rikken, C. W. T. Bulle-Lieuwma and D. C. Koningsberger, *J. Electrochem. Soc.*, 1989, **136**, 2914.
19. W.-Y. Lin, C. Wei and K. Rajeshwar, *J. Electrochem. Soc.*, 1993, **140**, 2477.
20. Y. Tak and K. Yong, *J. Phys. Chem. C*, 2008, **112**, 74.
21. N. S. Youssef, E. S. Kamel and M. M. Selim, *Bull. Soc. Chim. Fr.*, 1991, **12**, 648.
22. A. Mayer and D. A. Puotinen, *Nat. Bur. Stand.*, 1970, 431.
23. T. Hirakawa and Y. Nosaka, *Langmuir*, 2002, **18**, 3247.